Adaptive Field-of-view Restriction: Limiting Optical Flow to Mitigate Cybersickness in Virtual Reality

Fei Wu
wuxx1624@umn.edu
University of Minnesota
Minneapolis, MN, USA

Evan Suma Rosenberg
suma@umn.edu
University of Minnesota
Minneapolis, MN, USA

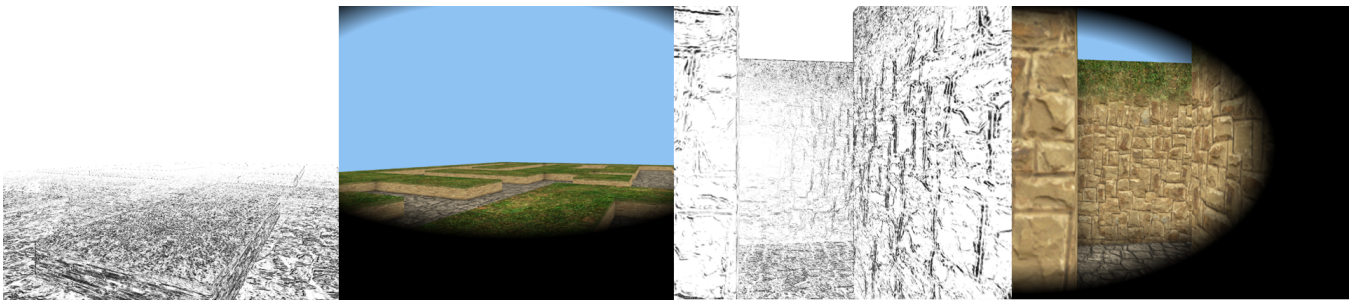

Figure 1: The adaptive restrictor is designed as a dynamic asymmetric mask to restrict the field-of-view in higher optical-flow regions when the user moves virtually. The two grayscale images show the optical flow patterns from wide open and close-quarter virtual environments, respectively. The color images show how the adaptive restrictor dynamically responds to occlude the regions with the most optical flow.

ABSTRACT

Dynamic field-of-view (FOV) restriction is a widely used software technique to mitigate cybersickness in commercial virtual reality (VR) applications. The classical FOV restrictor is implemented using a symmetric mask that occludes the periphery in response to translational and/or angular velocity. In this paper, we introduce adaptive field-of-view restriction, a novel technique that responds dynamically based on real-time assessment of optical flow generated by movement through a virtual environment. The adaptive restrictor utilizes an asymmetric mask to obscure regions of the periphery with higher optical flow during virtual locomotion while leaving regions with lower optical flow visible. To evaluate the proposed technique, we conducted a gender-balanced user study (N = 38) in which participants completed in a navigation task in two different types of virtual scenes using controller-based locomotion. Participants were instructed to navigate through either close-quarter or open virtual environments using adaptive restriction, traditional symmetric restriction, or an unrestricted control condition in three VR sessions separated by at least 24 hours. The results showed that the adaptive restrictor was effective in mitigating cybersickness and reducing subjective discomfort, while simultaneously enabling participants to remain immersed for a longer amount of time compared to the control condition. Additionally, presence ratings were significantly higher when using the adaptive restrictor compared to symmetric restriction. In general, these results suggest that adaptive field-of-view restriction based on real-time measurement of optical flow is a promising approach for virtual reality applications that seek to provide a better cost-benefit tradeoff between comfort and a high-fidelity experience.

CCS CONCEPTS

• **Human-centered computing** → **Virtual reality**; • **Computing methodologies** → **Virtual reality**; *Perception.*

KEYWORDS

Virtual reality, cybersickness, field-of-view, optical flow

ACM Reference Format:
Fei Wu and Evan Suma Rosenberg. 2022. Adaptive Field-of-view Restriction: Limiting Optical Flow to Mitigate Cybersickness in Virtual Reality. In *28th ACM Symposium on Virtual Reality Software and Technology (VRST '22), November 29-December 1, 2022, Tsukuba, Japan.* ACM, New York, NY, USA, 11 pages. https://doi.org/10.1145/3562939.3565611

1 INTRODUCTION

Virtual locomotion - the act of moving in virtual environments - is a fundamental interaction task in VR. However, The optical flow generated by locomotion can induce cybersickness in VR, especially when the user is only moving virtually, but not physically. The optical flow of imagery across the visual field is strongly associated with cybersickness and is a contributing factor to vection, which is the sensation of illusory self-motion in the absence of physical

VRST '22, November 29-December 1, 2022, Tsukuba, Japan

ACM ISBN 978-1-4503-9889-3/22/11.
https://doi.org/10.1145/3562939.3565611

movement [26]. The optical flow patterns in wide field-of-view displays can produce severe vection [19] that is inconsistent with the motion sensed by the vestibular system. Consequently, strong optical flow generated by virtual locomotion is often considered a major cause of cybersickness and could be further exacerbated by a wide field-of-view.

Field-of-view (FOV) plays an important role in perceiving optical flow. Studies have shown that motion at the periphery of the FOV is likely to produce more vection than motion at the center of the FOV [49]. To reduce the vection at the periphery, dynamic field-of-view restriction, also known as "tunneling," has been proposed and implemented in many commercial VR games [8]. This technique reduces cybersickness caused by visual information with the display of a black opaque texture that masks a portion of the user's visual field periphery. Multiple studies have shown that it holds promise for reducing discomfort associated with virtual locomotion [16, 52, 54]. Although it may be effective in mitigating cybersickness, FOV restriction could also potentially negatively affect the user's experience in VR. For example, previous research has shown that a wider FOV can improve user's immersion and task performance in virtual environments[12] and smaller FOV can negatively impact distance estimation[51], postural equilibrium[47], and the user's control of orientation [39].

Existing widely used implementations of FOV restriction often use a symmetric solid color or static mask to block the user's peripheral FOV [16]. However, this may result in sub-optimal occlusion of peripheral vision, and the vignette of the restrictor may expose the user to unnecessary optical flow. Moreover, the commonly used implementation is triggered by the user's forward and/or angular velocity, regardless of whether the optical flow in a scene is low or high. Reducing the FOV in scenes with minimal optical flow may not be necessary and could negatively impact the user's performance. An asymmetric restrictor that takes into consideration the amount of optical flow in different parts of the virtual scene to block only the regions of the virtual scene with the highest optical flow could overcome this limitation. To the best of our knowledge, no prior studies have been conducted to evaluate the effectiveness of asymmetric FOV restriction that dynamically adapts based on optical flow during virtual locomotion.

In this paper, we introduce *adaptive field-of-view restriction*, a novel technique that responds dynamically based on real-time optical flow generated by movement through a virtual environment. Adaptive FOV restriction is designed to be flexible for use in a wide variety of situations ranging from wide open spaces to close-quarter environments. To evaluate this technique, we conducted a user study in which participants completed in a navigation task in two different virtual scenes using controller-based locomotion. The experiment compared the adaptive restrictor, standard symmetric restrictor, and an unrestricted control condition in two different virtual scenes with optical flow patterns. The results showed that the adaptive restrictor was effective in reducing cybersickness and subjective discomfort compared to the control condition, while simultaneously providing a better sense of presence compared to the symmetric restrictor.

Figure 2: The standard symmetric FOV restriction technique uses a circular black mask to occlude the periphery. The inner and outer radii define the region in which the mask gradually transitions from fully transparent to fully opaque.

2 RELATED WORK

2.1 Optical Flow and Cybersickness

Cybersickness, also known as VR sickness, refers to a collection of negative symptoms experienced by users when using virtual reality systems. Cybersickness is often associated with motion sickness, although users may also experience a variety of symptoms including nausea, oculomotor discomfort, and disorientation. similar to those produced by other forms of motion sickness. Previous research has shown that users are more likely to suffer from cybersickness when they are exposed to moving visual content than when they are exposed to static content [9, 13, 29]. Sensory-conflict theory [40, 43] is a commonly cited explanation for this phenomenon. It claims that motion sickness is caused by a mismatch between the current sensory input patterns of the vestibular system regarding self-motion and the expected sensory input patterns generated by the visual system based on previous experiences. In the context of virtual reality, users often remain physically stationary but can see virtually moving images [19, 26], theoretically creating a visual-vestibular conflict. Although sensory conflict is an intuitive notion, the physiological causes of motion sickness are not fully understood. For example, the postural instability theory, which claims that the causative factor of motion sickness is the loss of postural control, also has considerable empirical support [41].

Regardless of its etiological causes, there exists substantial evidence that optical flow is a major contributing factor for visually induced motion sickness. Optical flow is generated by the stimulus of moving visual contents and allows users to experience illusory self-motion. The sensation of illusory self-motion in the absence of physical movement, known as vection [24, 37], is a significant contributor to motion sickness. Studies have found that users who experienced stronger vection also reported more severe cybersickness, and therefore vection might be used to identify those who are more susceptible [34, 42]. Optical flow of self-motion can induce vection and increases the probability of sickness in virtual environments; high rates of optical flow results in significantly higher rates of sickness [19], and this positive relationship is present in

Figure 3: The adaptive field-of-view restrictor is designed as an asymmetric mask that occludes the FOV in high optical-flow regions when the user moves virtually. Based on the image rendered to the screen, per-pixel optical flow is measured in real-time and pooled in a 32×32 grid. Image processing techniques are then used to detect regions of high optical flow and the size and shape of the FOV restrictor is adjusted dynamically.

both central and peripheral vision [27]. Studies showed that users' susceptibility to sickness can be reduced by gradual adaptation to increasing optic flow strength [1]. This may be due to the fact that optic flow stimuli can be sensitive to down-weight vestibular signals [17]. The relationship between optical flow and motion sickness has been extensively studied, and many parameters have been proposed to have an impact on the intensity of motion sickness induced by optical flow, such as the speed of virtual motion [44], the axis of motion [13], and the direction of optical flow [31].

The level of cybersickness can be measured using subjective or objective measurement techniques. Subjective measures rely on users' self-assessments, and the Kennedy-Lane Simulator Sickness Questionnaire (SSQ) is the most common instrument used to measure the severity of symptoms related to motion sickness [22]. The Fast Motion Sickness Score (FMS) is another measure commonly used to monitor the discomfort level of participants during a VR experience [23]. Although less common, some objective measures have also been applied in VR studies, such as postural sway [48], physiological signals [14], electrocardiogram (ECG), electrogastrogram (EGG), electroencephalograms (EEG), and heart rate.

2.2 Cybersickness Mitigation

Dynamic FOV restriction is a software technique that blocks the peripheral FOV in response to the user's linear or angular virtual velocity [8]. Also known as "tunneling" or "vignetting," FOV restriction is one of the most widely used methods to mitigate cybersickness during virtual locomotion in commercial applications [36]. This design is based on the assumption that the peripheral optical flow is an aggravating factor for motion sickness.

Several past studies have demonstrated that dynamic FOV restriction can reduce discomfort in head-mounted displays [5, 16, 18, 45]. It was also shown to be effective in mitigating VR sickness for both sexes [2, 4]. However, some studies of FOV restriction have shown opposite results. For example, cybersickness may be exacerbated by improperly occluding peripheral vision [32] or increasing and decreasing vignetting too frequently [35]. The results of previous experiments also revealed a mixed correlation between the degree of FOV restriction and subjective perception of presence. Cybersickness has a negative relationship with a user's sense of presence [50]. Although an effective cybersickness mitigation technique could potentially increase sense of presence, several previous experiments have found that dynamic FOV restriction either did not significantly affect presence [28, 45] or even potentially reduced it compared to an unrestricted FOV [5, 7]. One potential reason for this discrepancy could be that the mask blocked too much of the virtual environment, thereby contributing to a sense of unreality [45]. Research has also suggested that FOV restriction can come at the cost of users' task performance in spatial learning [7]. Taken together, these studies suggest that the specific implementation parameters for FOV restrictors are important and that a certain degree of peripheral vision should be maintained to balance the tradeoffs between cybersickness mitigation and a high-fidelity experience.

The standard implementation of FOV restriction uses a circular black mask that dynamically occludes the field-of-view based on the translational velocity and/or angular velocity of virtual movement. However, several recent studies have also investigated novel variants of dynamic FOV restriction, aiming to improve both user comfort and subjective experience, including: dynamic blurring in the retina's periphery, rather than using a black background [11, 28, 33], adjusting the FOV restrictor with the horizontal and vertical dimensions independently [25], displaying a wireframe model of the physical world in the periphery [53], tethering the center of the restrictor to eye motion [3], preserving the visibility of the ground plane when the restrictor displays [52], and asymmetrically restricting one side of the FOV during virtual turns [21, 54].

Several mitigation techniques have been proposed that manipulate optical flow patterns to reduce cybersickness. Buhler et al. evaluated two peripheral visual effects to reduce optical flow in the peripheral FOV with head-mounted displays [10]. Farmani et al. evaluated two discrete motion techniques aimed at reducing optical flow through inconsistent displacements [15]. Park et al. mixed the reverse optical flow visually with the virtual visual motion to reduce cybersickness [38]. Bala et al. utilized the amount of optical flow to determine the radius of field-of-view in 360° videos [6]. However, to our knowledge, real-time measurement of optical flow patterns as a mechanism for dynamically adjusting the size and shape of a FOV restrictor has not yet been investigated.

3 FIELD-OF-VIEW RESTRICTOR DESIGN

3.1 Symmetric FOV Restrictor Design

The symmetric FOV restrictor was implemented by extending VR Tunneling Pro, an open-source asset for the Unity game engine [46]. This framework provides a computationally lightweight restrictor using a symmetric circular mask that can be customized using a variety of parameters. The mask is defined by an outer radius and an inner radius, as shown in Figure 2. The peripheral FOV beyond the outer radius was completely obscured by a black opaque mask, while the region between the inner and outer radius provided a smooth transition from transparent to opaque. We modified the

Algorithm 1 A pipeline to create adaptive field-of-view restriction

1: Compute the optical flow in the x and y directions using a simplified version of the Horn–Schunck algorithm optimized for use in a real-time shader and output the optical flow texture [20, 30].
2: Divide the optical flow texture into 32×32 grids (1024 grids in total) and use the maximum optical flow value within each grid to represent the optical flow value of this grid. The output is a 32×32 ARGB texture.
3: **for** Each pixel in the texture **do**
4: **if** pixel's optical flow < threshold **then**
5: The alpha channel of the pixel is 0
6: **else**
7: The alpha channel of the pixel is 1
8: Use the connected-component labelling to connect pixels with alpha channel equal to 0.
9: Find the largest connected region.
10: Approximate the largest connected region as an ellipse region and calculate the center c and approximate radius r of the region.
11: $c_x = Clamp(c_x, c_{screen_x} - c_{offset_l}, c_{screen_x} + c_{offset_r})$
12: $c_y = Clamp(c_y, c_{screen_y} - c_{offset_d}, c_{screen_y} + c_{offset_u})$
13: **if** $c_{screen_x} > c_x$ **then**
14: $x_{offset} = (c_{screen_x} - c_x)/c_{offset_l}$
15: **else**
16: $x_{offset} = (c_{screen_x} - c_x)/c_{offset_r}$
17: **if** $c_{screen_y} > c_y$ **then**
18: $y_{offset} = (c_{screen_y} - c_y)/c_{offset_d}$
19: **else**
20: $y_{offset} = (c_{screen_y} - c_y)/c_{offset_u}$
21: Calculate the minimum restrictor radius r_{min} based on the restrictor center c using the following equation $r_{min} = w \cdot \sqrt{c^2_{offset_x} + c^2_{offset_y}} \cdot r_{min}$
22: Calculate the restrictor radius $r = max(r, r_{min})$
23: Apply r as the inner radius of the restrictor, then add 0.1 to form the outer radius.

default method of measuring the mask radius in screen space to angular FOV so that our results could be more easily interpreted and consistently implemented on various headsets.

The symmetric restrictor was activated whenever the user initiated either a virtual translation or rotation. When the movement conditions are met, the size of the restrictor was dynamically scaled from the maximum FOV to a preset minimum degree. We selected parameters that were similar to those used in commercial applications and refined them through extensive pilot testing with multiple users. In this experiment, the outer radius of the FOV restrictor was set to 60° and the inner radius was set to 55°. The FOV restrictor was dynamically scaled over a duration of 0.25 seconds when participants started or stopped moving.

3.2 Adaptive FOV Restrictor Design

An overview of the adaptive restrictor pipeline is shown in Figure 3, and a more detailed description is provided in Algorithm 1. Similar to the standard symmetric restrictor, adaptive restriction was invoked during virtual locomotion and was not displayed when users were physically moving only. The optical flow was measured once per frame, and the FOV parameters were dynamically smoothed over a time window of 0.5 seconds. The parameters in each step were selected based on their performance in pilot testing so that they provided a comfortable experience for the user.

The algorithm defines the following variables: c, a 2D vector (c_x, c_y), representing the center of the restrictor in the x and y direction; r, a 2D vector (r_x, r_y) representing the radius in x and y direction; c_{offset}, a 4D vector $(c_{offset_u}, c_{offset_d}, c_{offset_l}, c_{offset_r})$, representing center offset in up, down, left and right directions; r_{min}, a 2D vector (r_{min_x}, r_{min_y}), representing the minimum restrictor radius in x and y directions; c_{screen}, a 2D vector $(c_{screen_x}, c_{screen_y})$, representing the screen center; and w, a weight variable. We applied $w = 1$ in our implementation.

The input for optical flow detection were images of the viewpoint generated based on the view and projection matrices of the monoscopic virtual camera. The threshold in step 4 was determined through pilot testing with multiple users to ensure that the region of maximum optical flow can be selected and that the restrictor would not block too much of the user's vision. Subsequent pilot testing was also conducted to confirm that the selected parameters provide a comfortable user experience. To avoid jitter, we also applied a smoothing process to both the center and the radius of the restrictor. Additionally, to avoid cases where the restrictor center would be too heavily offset towards the boundary, resulting in a very small viewing area, we added steps 15-25 to adjust the minimum radius of the restrictor by the maximum offset of its center. The larger the center offset, the larger the minimum radius; conversely, the smaller the center offset, the smaller the minimum radius.

4 USER STUDY

4.1 Experiment Design

In the experiment, the goal was to evaluate and compare the effectiveness of three different FOV restriction conditions (no restriction, symmetric restriction, adaptive restriction) in two different virtual scenes (close-quarter and open environments). The study used a mixed design with restriction technique as a within-subjects variable and virtual scene as a between-subjects variable. Participants experienced the restrictors in separate VR sessions, each of which was separated by at least 24 hours to avoid the compounding effects of cybersickness. The order of within-subjects trials was counterbalanced using a Latin Square design. For the virtual scenes, participants were divided into two groups, one experiencing the close-quarter environment and the rest experiencing the open environment. This experiment was conducted in our laboratory, and the study protocol was reviewed and approved by our University's Institutional Review Board (IRB).

4.2 Participants

Participants were recruited through the university. They were required to have a normal or corrected-to-normal vision and be able to communicate in spoken and written English. Participants that were pregnant or had a history of epilepsy or severe motion sickness were instructed not to participate due to safety concerns. Each

(a) (b)

Figure 4: (a) A partial overhead view of the virtual maze, which contains complex pathways and frequent turns. (b) To complete the task, participants collected the gold coins by traveling over them.

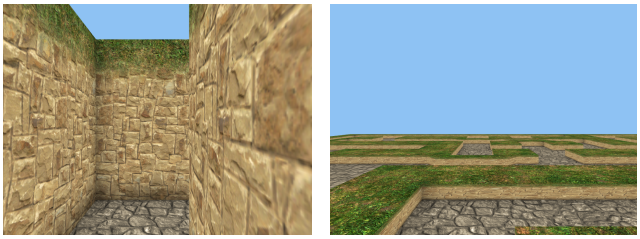

(a) (b)

Figure 5: Screenshots of the close-quarter (a) and open environments (b). The layout of both scenes was consistent and only differed in wall height, which resulted in drastically different optical flow patterns from similar virtual paths.

participant was compensated with a $20 Amazon gift card upon finishing all three sessions. A total of 38 participants completed the study (19 male, 19 female). Participant ages ranged from 19 to 27 years old ($M = 22$, $SD = 2.46$) with a variety of video game experience, ranging from little to over 10 years of gaming experience.

4.3 Equipment

Participants experienced the virtual environment using a Vive Pro Eye and Valve Index controllers. The headset provides a stereoscopic view with a resolution of 1440×1600 per eye, a refresh rate of 90Hz, and a field-of-view of approximately 110°. The experiment was run on an Intel Core i7-7820HK 2.90GHz PC running Windows 10 with 16 GB of RAM and an NVIDIA GeForce GTX 1080 graphics card. The virtual environment was implemented in Unity 2019.4.29f1. During the study, we recorded the frame rate on the Vive Pro Eye for each participant and observed that it was able to stay approximately equal to the device's maximum refresh rate of 90hz.

4.4 Virtual Environment

The wall height was the only difference between the two environments. The close-quarter environment had 3 meters high walls, and the open environment had 0.15 meter high walls (see Figure 5) .

4.5 Procedure

Because cybersickness can potentially persist for hours after exposure [40], participants came to our lab for three separate sessions separated by at least 24 hours. At the beginning of the first session, participants read the information sheet, were instructed on the task, and learned how to use the controller. Afterwards, they immersed themselves in the virtual environment and completed the Simulator Sickness Questionnaire (SSQ) [22]. After filling in the questionnaire, each participant performed a practice trial to ensure that they understood the control mechanisms of the virtual environment.

Participants were instructed to stand during the virtual reality experience. They were able to virtually move forward/backward and turn virtually via the thumbstick on a Valve Index controller using view-directed steering. Forward velocity was 2.5 meters per second, and angular velocity was 45° per second. The velocity parameters were constant and determined through extensive pilot testing to determine a good balance between comfort and responsiveness. Participants were also able to physically rotate their heads, but were instructed not to walk physically.

After the practice trial finished, participants then completed 10 experimental trials, each of which was designed to take approximately two minutes, resulting in an overall immersion time of about 20 minutes. Participants were required to follow a path through the maze defined by the gold coins, as described in Section 4.4. At the end of each trial, participants reached a checkpoint and were instructed to rate their subjective discomfort level on a scale from 0 to 10 (see Figure 6), following a similar procedure to the seminal FOV restrictor study by Fernandes and Feiner [16]. Participants were instructed at the beginning that the navigation task would be stopped immediately if they reported a discomfort score of 10. Participants were also able to quit immediately via a spatial menu that was opened using the controller's grip button.

During each trial, the virtual reality application collected information, including discomfort score for each trial, position and orientation data for each frame, the overall task duration, the number of completed trials, and the size of the displayed FOV. Upon completing or terminating the navigation task, the participants completed the SSQ post-test and a feedback questionnaire. At the end of the third session, the participants also needed to complete a demographic questionnaire. Each session was designed to take approximately 25 - 30 minutes to complete all procedures, including pre- and post-questionnaires.

5 MEASURES

The performance of the three FOV restriction conditions was evaluated using the following metrics.

Cybersickness. The Simulator Sickness Questionnaire (SSQ) scores were calculated using the deltas between participants' responses to the SSQ before and after each session of the study. This is a standard questionnaire to assess the extent of each symptom associated with cybersickness.

Discomfort Scores. We adopted the metrics proposed by Fernandes and Feiner [16] to process the discomfort score and calculate

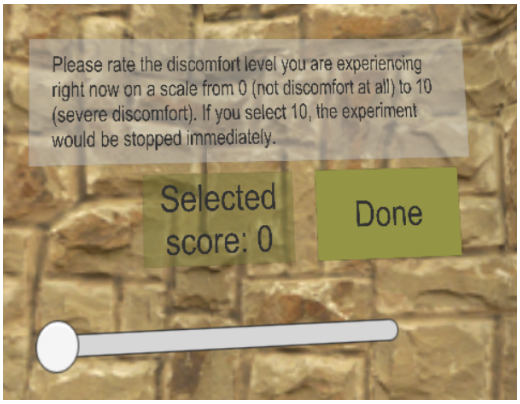

Figure 6: Participants used a spatial menu to rate their discomfort level on a 0-10 scale at checkpoints throughout the experimental task.

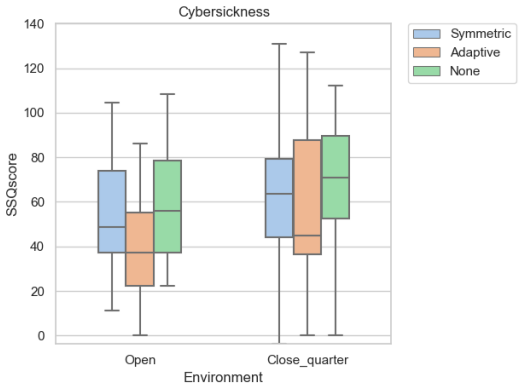

Figure 7: Box plots of the delta SSQ scores for each condition. Users reported significantly lower delta SSQ score when using the Adaptive restrictor compared to the None condition.

two variables: the participant's time-weighted *Average Discomfort Score (ADS)* and the *Relative Discomfort Score (RDS)*.

$$RDS = \frac{\sum_{0 \le i \le t_{stop}} DS_i + (t_{max} - t_{stop} + 1) DS_{stop}}{t_{max}} \quad (1)$$

$$ADS = \frac{\sum_{0 \le i \le t_{stop}} DS_i}{N} \quad (2)$$

The amount of time each participant immersed in the virtual environment was t_{stop}. The longest one was t_{max}. The discomfort score at t_{stop} was recorded as DS_{stop}. DS_i was the discomfort score at each second i prior to t_{stop}. If a participant terminated before t_{max}, their DS_{stop} was recorded as 10 and repeated each second from the terminated time until t_{max}. If a participant finished early with a discomfort score less than 10, their final score was used as DS_{stop} and repeated. N was the number of trials completed. This two metrics rated the participants' general level of discomfort rather than specific symptoms, and are therefore a distinct, yet complementary, measure from the SSQ scores.

Task Performance. The task was terminated immediately if the participant selected a discomfort level of 10 or used the button to quit the game. Thus, the overall immersion time in the virtual environment could be expected to be an objective indicator of cybersickness to some extent. The duration, defined as the time from when the participant enters the first trial to the completion or exit of the game, and the number of completed trials were automatically recorded by the system. In addition, although the velocity and angular velocity were constant during the navigation task, participants would stop more frequently to take a break if they had stronger cybersickness. Therefore, the average time they spent in each trial was calculated using the following equation:

$$\text{average time per trial} = \frac{\text{total duration}}{\text{number of completed trials}} \quad (3)$$

Only data from participants who completed at least one trial were used to calculate the average time per trial.

Subjective Experience. The feedback questionnaire asked participants to rate their agreement with the following two statements on a 7-point Likert scale:

(1) It was difficult to see the virtual environment during locomotion.
(2) I had a sense of being present in the virtual environment.

The first measure was referred to as *visibility*, and its score was reversed so that higher scores are associated with positive findings. The second measure was referred to as *presence* in the results. It should be noted that we only used a single question to assess presence instead of a longer format questionnaire because this was only a tertiary measure and we were concerned with limiting overall participation to less than 90 minutes across the three sessions.

6 HYPOTHESES

Symmetric FOV restriction has been shown to effectively reduce discomfort, but this simplistic implementation may result in over-restriction that negatively impacts other aspects of the subjective user experience. Our goal in developing the adaptive restrictor, therefore, was to provide a superior benefits with less severe trade-offs. To this end, we formulated the following five scientific hypotheses:

- H1: Participants would report lower delta SSQ scores with the adaptive and symmetric restrictors compared to the control condition without restriction.
- H2: Participants would report lower discomfort scores with the adaptive and symmetric restrictors compared to the control condition.
- H3: Participants would be immersed in the navigation task longer with the adaptive restrictor and symmetric restrictor compared to the control condition.
- H4: Participants would report better visibility with the adaptive restrictor and control condition compared to the symmetric restrictor.

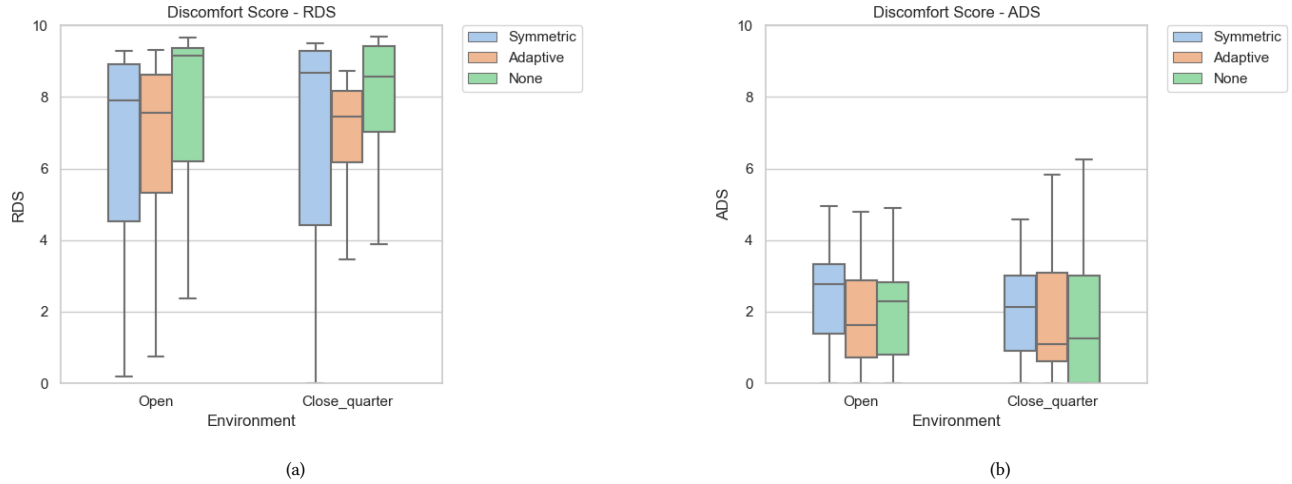

(a) (b)

Figure 8: (a) Box plots of relative discomfort scores (RDS) for each condition per environment. (b) Box plots of average discomfort scores (ADS) for each condition per environment. A value of 0 represents "no discomfort at all" and increasing numbers correspond to greater discomfort. Users reported significantly lower RDS when using the Adaptive restrictor and Symmetric restrictor compared to the None condition.

- H5: Participants would report a greater sense of presence with the adaptive restrictor and control condition compared to the symmetric restrictor.

7 RESULTS

Shapiro-Wilk tests indicated violations of normality for cybersickness, discomfort, and task performance measures. Therefore, all variables were analyzed using non-parametric tests, and descriptive statistics are reported as median (*Mdn*) and interquartile range (*IQR*). Friedman tests were conducted using a significance value of $\alpha = .05$. When significant differences were found, post-hoc analyses were conducted using Conover tests with a Holm-Bonferroni correction for multiple comparisons. Because no significant effects were found between the two virtual environment types across all our measures, these analyses were not included in our results.

Cybersickness. Results for the delta overall SSQ scores are shown in Figure 7. A Friedman test revealed a significant difference among the three FOV conditions, $\chi^2(2) = 8.78$, $p = .01$. Post hoc analysis showed that the Adaptive Restrictor ($Mdn = 41.14$, $IQR = 53.29$) resulted in significantly lower delta SSQ scores compared with the None condition ($Mdn = 71.06$, $IQR = 37.40$), $p = .01$. The Symmetric restrictor ($Mdn = 57.97$, $IQR = 41.14$) was not significantly different from the None condition, $p = .31$, or the Adaptive restrictor, $p = .12$. These results partially support hypothesis H1.

Discomfort Scores. Results for the average and relative discomfort scores are shown in Figure 8. Analysis of ADS ratings using a Friedman test did not reveal any significant differences among the three FOV conditions, $\chi^2(2) = 1.02, p = .60$. However, for RDS ratings, the analysis was significant, $\chi^2(2) = 20.16$, $p < .001$. Post hoc comparisons indicated that the Adaptive restrictor ($Mdn = 7.48$, $IQR = 3.13$) was significantly more comfortable than the None condition ($Mdn = 9.04$, $IQR = 2.71$), $p < .001$. The Symmetric condition ($Mdn = 8.53$, $IQR = 4.62$) was also more comfortable than the None condition, $p = .01$. However, RDS ratings for the Adaptive and the Symmetric restrictors were not significantly different, $p = .14$. The relative discomfort score results support hypothesis H2.

Task Performance. Results for overall task duration and average time per trial are shown in Figure 9. A Friedman test for task duration revealed significant differences among the three FOV conditions, $\chi^2(2) = 9.53$, $p < .01$. Post hoc comparisons indicated participants remained immersed in the navigation task significantly longer using the Adaptive restrictor ($Mdn = 618.36$, $IQR = 747.58$) compared to the None condition ($Mdn = 299.60$, $IQR = 865.18$), $p = .01$. The Symmetric restrictor ($Mdn = 490.79$, $IQR = 1015.26$) was not significantly different from either the Adaptive restrictor, $p = .43$, or the None condition, $p = .06$.

A Friedman test for average times spent to complete each trial was not significant, $\chi^2(2) = 2.39$, $p = .30$. However, for the number of completed trials, this analysis revealed significant differences among the three FOV conditions, $\chi^2(2) = 17.56$, $p < .001$. Post hoc comparisons indicated that compared to the None condition, participants completed significantly more trials when using either the Adaptive restrictor, $p < .001$, or the Symmetric restrictor, $p = .03$. The Adaptive and Symmetric restrictor conditions were not significantly different, $p = 0.09$. Taken together, these results partially support hypothesis H3.

Subjective Experience. Results from the feedback questionnaire are shown in Figure 10. A Friedman test revealed significant differences in visibility ratings among the three FOV conditions, $\chi^2(2) = 22.97$, $p < .001$. Post-hoc analysis indicated that visibility ratings were higher in the None condition ($Mdn = 6.00$, $IQR = 1.00$) compared to both the Adaptive restrictor ($Mdn = 4.00$, $IQR = 2.00$),

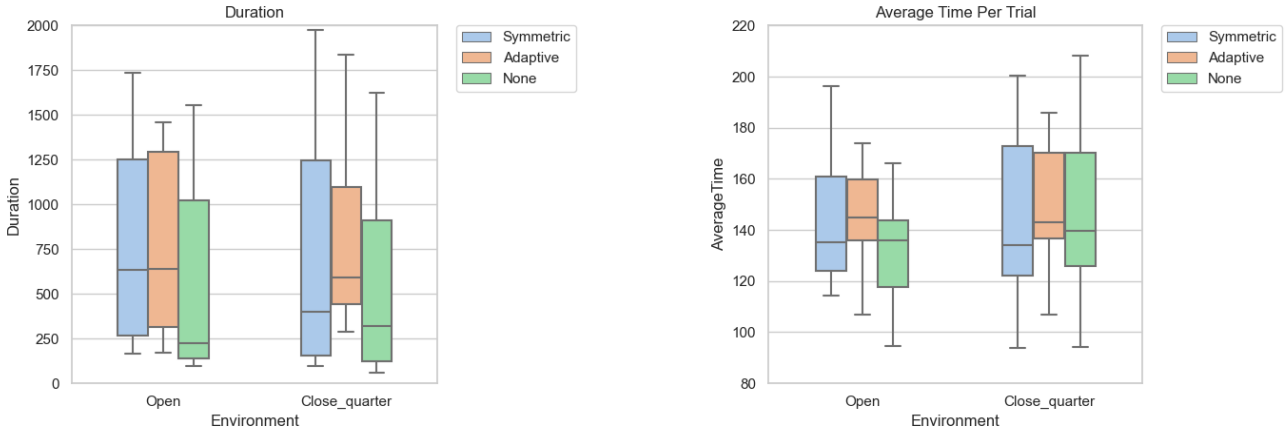

(a) (b)

Figure 9: (a) Box plots of immersion duration for each condition. (b) Box plots of average immersion time in each trial for each condition. Participants using the adaptive restrictor persisted significantly longer in the virtual environment compared to the unrestricted condition.

p =< .001, and Symmetric restrictor (Mdn = 3.00, IQR = 2.75), p =< .001. However, the difference between the Adaptive and Symmetric restrictors was not significant, p = .58. These results partially support hypothesis H4.

A Friedman test of the presence ratings also revealed significant differences among the three FOV conditions, $\chi^2(2) = 17.40$, $p < .001$. Post-hoc analysis indicated that the Symmetric restrictor (Mdn = 4.00, IQR = 1.75) received significantly lower presence ratings compared to both the Adaptive restrictor (Mdn = 5.50, IQR = 1.00), $p < .01$, and the None condition (Mdn = 6.00, IQR = 1.00), $p < .001$. Presence ratings for the Adaptive restrictor and None condition were not significantly different, p = .28. These results fully support hypothesis H5.

8 DISCUSSION

8.1 Effects on Cybersickness and Discomfort

The results for both the delta SSQ scores and relative discomfort ratings indicated that the adaptive restrictor was effective in mitigating negative symptoms compared to the control condition without FOV restriction. Because both restrictor conditions restrict the optical flow visible to the participant during virtual movement, we did not have any a priori hypotheses that one would outperform the other on comfort measures. Although it is interesting to note that SSQ scores for the symmetric restrictor were generally observed to lie in between the adaptive and control conditions, these results were statistically inconclusive, and no scientific conclusions can be drawn from these data. These results are also consistent with the original FOV restriction experiment reported by Fernandes and Feiner, in which the symmetric restrictor provided benefits for relative discomfort ratings, but not SSQ scores [16].

Since average discomfort scores were computed from only the trials that were completed, a participant who quit early may have scores that are not directly comparable to a participant who finished all trials. Therefore, the ADS is only meaningful if most of the participants completed a consistent number of trials. Given the wide distribution of the number of trials completed by participants in our experiment, the relative discomfort scores provide a more reliable basis for comparison. These results are consistent with prior studies (e.g., [16, 52, 54]) and provide further evidence that it may not be useful to analyze ADS in future experiments using this protocol unless all participants complete the same number of trials.

8.2 Effects on Task Performance

Participants using the adaptive restrictor remained immersed for significantly longer in the virtual environment than the unrestricted condition. Because participants were explicitly instructed to stop if they felt motion sickness and the task ended immediately upon entering a discomfort score of 10, the longer immersion time was further evidence that the adaptive restrictor was effective in mitigating negative effects. In addition, no significant effects were found for the three restriction conditions in the average time participants took to complete each trial, so we did not find any empirical evidence supporting an alternative explanation based on differences in movement speed through the maze.

8.3 Effects on Subjective Experience

Participants rated their visibility significantly higher in the unrestricted control condition compared to both the adaptive and symmetric restrictors. This is an expected result, because the use of FOV restriction necessarily entails finding an acceptable tradeoff between visibility and discomfort. Although the subjective ratings of visibility between the two restrictors were not significant, the adaptive restrictor produced significantly higher presence ratings. This is an encouraging result that may be explained by examining the quantitative logs of the displayed FOV during each frame. When

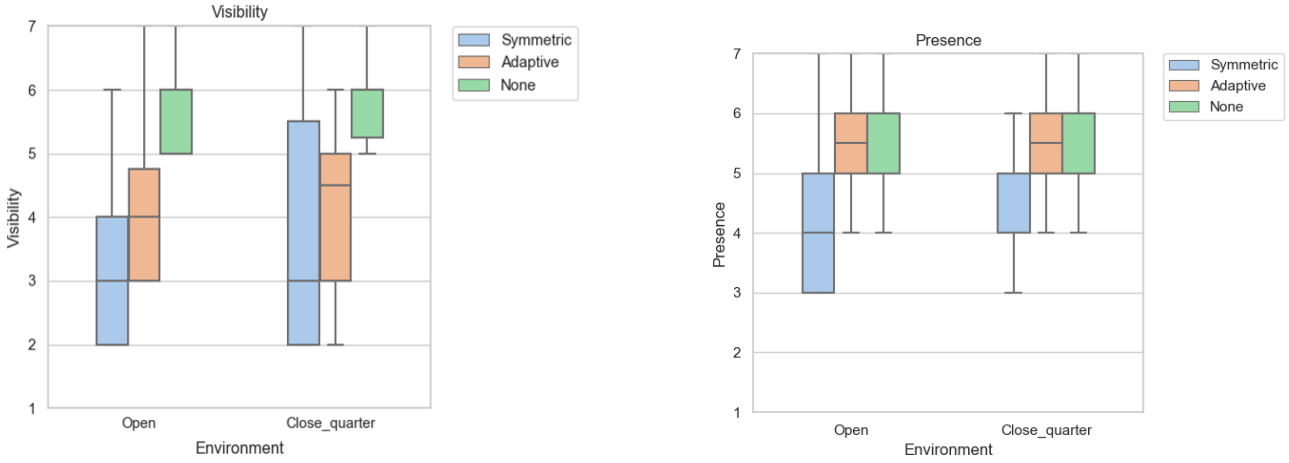

(a) (b)

Figure 10: (a) Box plots of the visibility. The direction of the scale was adjusted so that higher values are associated with positive outcomes. Users reported significantly better visibility when using unrestricted condition compared to the Adaptive restrictor and the Symmetric restrictor. (b) Box plots of the sense of presence. Users reported a significantly higher sense of presence when using the Adaptive restrictor and unrestricted condition compared to the Symmetric restrictor.

the adaptive restricor was applied, participants were shown a median value of 90.88° horizontal FOV and 90.87° vertical FOV in the close-quarter environment. In the open environment, the median value was 94.40° for the horizontal FOV and 78.54° for the vertical FOV. Because the symmetric restrictor provided approximately 60° FOV in both environments, the adaptive restrictor occluded less of the visual field while providing similar benefits in mitigating cybersickness and general discomfort.

8.4 Limitations

The adaptive restriction technique has several limitations that may be addressed in future work. Consistent with prior implementations of FOV restriction, the occluding mask was shaped as an ellipse. However, the boundaries between the regions with the high and low optical flow may form an irregular shape within the user's visual field, and an ellipse may not an ideal geometric approximation. On the other hand, a mask that more precisely fits within the low optical flow regions can have complex, non-convex contours, which may result in undesirable visual artifacts. In general, the effects of non-elliptical FOV restrictors have not been investigated and remain an open question for future work.

In this study, the center of the adaptive restrictor was changed based on the optical flow computed from the visual scene. Our implementation is compatible with a wide variety of consumer VR systems, and we imposed general constraints on the restrictor size and position to prevent it from shifting too far from the center or blocking too much of the visual field. However, when targeting a headset with real-time eye tracking, we believe that adaptive restriction could be further improved by considering the user's gaze direction in combination with optical flow.

9 CONCLUSION

In this paper, we proposed and evaluated adaptive FOV restriction, a novel variant of a widely used technique for mitigating cybersickness in virtual reality applications. We conducted a mixed design user study with three conditions and two environments to compare the proposed technique with a traditional symmetric restrictor and a control condition without FOV restriction. The results indicated that adaptive restrictor was effective in mitigating cybersickness and reducing subjective discomfort compared to the unrestricted control condition, while simultaneously supporting a better sense of presence than the symmetric restrictor. Therefore, we conclude that adaptive FOV restriction based on real-time measurement of optical flow is a promising approach, especially for virtual reality applications that involve transitioning between indoor and outdoor scenes with varying visual characteristics.

In the future, we plan to further investigate novel variants and parameters for FOV restriction techniques capable of adapting themselves to virtual environments or to individual users. For example, there are a variety of objective measures that can be used as input to adjust the FOV restriction size, such as postural sway, electrodermal activity, heart rate. and electroencephalogram data. In general, the design space of FOV restriction techniques has not yet been exhaustively explored, and future studies comparing different variants of asymmetric and adaptive restrictors are needed to improve scientific understanding of their impact on the user experience and establish design guidelines for their practical use.

ACKNOWLEDGMENTS

This material is based upon work supported by the National Science Foundation under Grant No. 1901423. The authors would also like to thank Isayas Adhanom for his assistance in revising the paper.

REFERENCES

[1] Isayas Adhanom, Savannah Halow, Eelke Folmer, and Paul MacNeilage. 2022. VR Sickness Adaptation with Ramped Optic Flow Transfers from Abstract To Realistic Environments. *Frontiers in Virtual Reality* (2022), 60.

[2] Isayas Berhe Adhanom, Majed Al-Zayer, Paul Macneilage, and Eelke Folmer. 2021. Field-of-view restriction to reduce VR sickness does not impede spatial learning in women. *ACM Transactions on Applied Perception (TAP)* 18, 2 (2021), 1–17.

[3] Isayas Berhe Adhanom, Nathan Navarro Griffin, Paul MacNeilage, and Eelke Folmer. 2020. The Effect of a Foveated Field-of-view Restrictor on VR Sickness. In *2020 IEEE Conference on Virtual Reality and 3D User Interfaces (VR)*. IEEE, 645–652.

[4] Majed Al Zayer, Isayas B Adhanom, Paul MacNeilage, and Eelke Folmer. 2019. The effect of field-of-view restriction on sex bias in vr sickness and spatial navigation performance. In *Proceedings of the 2019 CHI Conference on Human Factors in Computing Systems*. 1–12.

[5] Paulo Bala, Dina Dionísio, Valentina Nisi, and Nuno Nunes. 2018. Visually induced motion sickness in 360° videos: Comparing and combining visual optimization techniques. In *2018 IEEE International Symposium on Mixed and Augmented Reality Adjunct (ISMAR-Adjunct)*. IEEE, 244–249.

[6] Paulo Bala, Ian Oakley, Valentina Nisi, and Nuno Nunes. 2020. Staying on track: a comparative study on the use of optical flow in 360 video to mitigate vims. In *ACM International Conference on Interactive Media Experiences*. 82–93.

[7] Erica M Barhorst-Cates, Kristina M Rand, and Sarah H Creem-Regehr. 2016. The effects of restricted peripheral field-of-view on spatial learning while navigating. *PloS one* 11, 10 (2016), e0163785.

[8] Mark Bolas, J Adam Jones, Ian McDowall, and Evan Suma. 2017. Dynamic field of view throttling as a means of improving user experience in head mounted virtual environments. US Patent 9,645,395.

[9] Frederick Bonato, Andrea Bubka, Stephen Palmisano, Danielle Phillip, and Giselle Moreno. 2008. Vection change exacerbates simulator sickness in virtual environments. *Presence: Teleoperators and Virtual Environments* 17, 3 (2008), 283–292.

[10] Helmut Buhler, Sebastian Misztal, and Jonas Schild. 2018. Reducing vr sickness through peripheral visual effects. In *2018 IEEE Conference on Virtual Reality and 3D User Interfaces (VR)*. IEEE, 517–9.

[11] Kieran Carnegie and Taehyun Rhee. 2015. Reducing visual discomfort with HMDs using dynamic depth of field. *IEEE computer graphics and applications* 35, 5 (2015), 34–41.

[12] Polona Caserman, Augusto Garcia-Agundez, Alvar Gámez Zerban, and Stefan Göbel. 2021. Cybersickness in current-generation virtual reality head-mounted displays: systematic review and outlook. *Virtual Reality* 25, 4 (2021), 1153–1170.

[13] Wanjun Chen, JZ Chen, and Richard Hau Yue So. 2011. Visually induced motion sickness: Effects of translational visual motion along different axes. *Contemporary ergonomics and human factors* 2011 (2011), 281–287.

[14] Mark S Dennison, A Zachary Wisti, and Michael D'Zmura. 2016. Use of physiological signals to predict cybersickness. *Displays* 44 (2016), 42–52.

[15] Yasin Farmani and Robert J Teather. 2020. Evaluating discrete viewpoint control to reduce cybersickness in virtual reality. *Virtual Reality* 24, 4 (2020), 645–664.

[16] Ajoy S Fernandes and Steven K Feiner. 2016. Combating VR sickness through subtle dynamic field-of-view modification. In *2016 IEEE Symposium on 3D User Interfaces (3DUI)*. IEEE, 201–210.

[17] Maria Gallagher, Reno Choi, and Elisa Raffaella Ferrè. 2020. Multisensory interactions in virtual reality: optic flow reduces vestibular sensitivity, but only for congruent planes of motion. *Multisensory research* 33, 6 (2020), 625–644.

[18] Colin Groth, Jan-Philipp Tauscher, Nikkel Heesen, Steve Grogorick, Susana Castillo, and Marcus Magnor. 2021. Mitigation of Cybersickness in Immersive 360 Videos. In *2021 IEEE Conference on Virtual Reality and 3D User Interfaces Abstracts and Workshops (VRW)*. IEEE, 169–177.

[19] Lawrence J Hettinger and Gary E Riccio. 1992. Visually induced motion sickness in virtual environments. *Presence: Teleoperators & Virtual Environments* 1, 3 (1992), 306–310.

[20] Berthold KP Horn and Brian G Schunck. 1981. Determining optical flow. *Artificial intelligence* 17, 1-3 (1981), 185–203.

[21] IGN. Accessed: 2021-03-17. Eagle Flight Review. https://www.youtube.com/watch?v=W2LrzcZCBOE.

[22] Robert S Kennedy, Norman E Lane, Kevin S Berbaum, and Michael G Lilienthal. 1993. Simulator sickness questionnaire: An enhanced method for quantifying simulator sickness. *The international journal of aviation psychology* 3, 3 (1993), 203–220.

[23] Behrang Keshavarz and Heiko Hecht. 2011. Validating an efficient method to quantify motion sickness. *Human factors* 53, 4 (2011), 415–426.

[24] Behrang Keshavarz, Bernhard E Riecke, Lawrence J Hettinger, and Jennifer L Campos. 2015. Vection and visually induced motion sickness: how are they related? *Frontiers in psychology* 6 (2015), 472.

[25] Sehoon Kim, Seungheon Lee, Nupur Kala, Jaesung Lee, and Wonhee Choe. 2018. An effective FoV restriction approach to mitigate VR sickness on mobile devices. *Journal of the Society for Information Display* 26, 6 (2018), 376–384.

[26] Joseph J LaViola Jr. 2000. A discussion of cybersickness in virtual environments. *ACM Sigchi Bulletin* 32, 1 (2000), 47–56.

[27] Jiun-Yu Lee, Ping-Hsuan Han, Ling Tsai, Rih-Ding Peng, Yang-Sheng Chen, Kuan-Wen Chen, and Yi-Ping Hung. 2017. Estimating the simulator sickness in immersive virtual reality with optical flow analysis. In *SIGGRAPH Asia 2017 Posters*. 1–2.

[28] Yun-Xuan Lin, Rohith Venkatakrishnan, Roshan Venkatakrishnan, Elham Ebrahimi, Wen-Chieh Lin, and Sabarish V Babu. 2020. How the Presence and Size of Static Peripheral Blur Affects Cybersickness in Virtual Reality. *ACM Transactions on Applied Perception (TAP)* 17, 4 (2020), 1–18.

[29] Astrid JA Lubeck, Jelte E Bos, and John F Stins. 2015. Motion in images is essential to cause motion sickness symptoms, but not to increase postural sway. *Displays* 38 (2015), 55–61.

[30] mattatz. Accessed: 2022-01-14. unity-optical-flow. https://github.com/mattatz/unity-optical-flow.

[31] Alireza Mazloumi Gavgani, Deborah M Hodgson, and Eugene Nalivaiko. 2017. Effects of visual flow direction on signs and symptoms of cybersickness. *PloS one* 12, 8 (2017), e0182790.

[32] Jason D Moss and Eric R Muth. 2011. Characteristics of head-mounted displays and their effects on simulator sickness. *Human factors* 53, 3 (2011), 308–319.

[33] Guang-Yu Nie, Henry Been-Lirn Duh, Yue Liu, and Yongtian Wang. 2019. Analysis on Mitigation of Visually Induced Motion Sickness by Applying Dynamical Blurring on a User's Retina. *IEEE transactions on visualization and computer graphics* (2019).

[34] Suzanne AE Nooij, Paolo Pretto, Daniel Oberfeld, Heiko Hecht, and Heinrich H Bülthoff. 2017. Vection is the main contributor to motion sickness induced by visual yaw rotation: Implications for conflict and eye movement theories. *PloS one* 12, 4 (2017), e0175305.

[35] Nahal Norouzi, Gerd Bruder, and Greg Welch. 2018. Assessing vignetting as a means to reduce VR sickness during amplified head rotations. In *Proceedings of the 15th ACM Symposium on Applied Perception*. 1–8.

[36] Oculus. Accessed on 10-22-2021. Reduce Optic Flow. https://developer.oculus.com/resources/locomotion-design-reduce-optic-flow/.

[37] Stephen Palmisano, Robert S Allison, Mark M Schira, and Robert J Barry. 2015. Future challenges for vection research: definitions, functional significance, measures, and neural bases. *Frontiers in psychology* 6 (2015), 193.

[38] Su Han Park, Bin Han, and Gerard Jounghyun Kim. 2022. Mixing in reverse optical flow to mitigate vection and simulation sickness in virtual reality. In *CHI Conference on Human Factors in Computing Systems*. 1–11.

[39] Robert Patterson, Marc D Winterbottom, and Byron J Pierce. 2006. Perceptual issues in the use of head-mounted visual displays. *Human factors* 48, 3 (2006), 555–573.

[40] Lisa Rebenitsch and Charles Owen. 2016. Review on cybersickness in applications and visual displays. *Virtual Reality* 20, 2 (2016), 101–125.

[41] Gary E Riccio and Thomas A Stoffregen. 1991. An ecological theory of motion sickness and postural instability. *Ecological psychology* 3, 3 (1991), 195–240.

[42] Dante Risi and Stephen Palmisano. 2019. Effects of postural stability, active control, exposure duration and repeated exposures on HMD induced cybersickness. *Displays* 60 (2019), 9–17.

[43] Sarah Sharples, Sue Cobb, Amanda Moody, and John R Wilson. 2008. Virtual reality induced symptoms and effects (VRISE): Comparison of head mounted display (HMD), desktop and projection display systems. *Displays* 29, 2 (2008), 58–69.

[44] Richard HY So, WT Lo, and Andy TK Ho. 2001. Effects of navigation speed on motion sickness caused by an immersive virtual environment. *Human factors* 43, 3 (2001), 452–461.

[45] Joel Teixeira and Stephen Palmisano. 2021. Effects of dynamic field-of-view restriction on cybersickness and presence in HMD-based virtual reality. *Virtual Reality* 25, 2 (2021), 433–445.

[46] Luke Thompson. 2017. VR Tunnelling Pro. http://www.sigtrapgames.com/VrTunnellingPro/html/. Accessed on 12-01-2020.

[47] Kathleen Turano, Susan J Herdman, and Gislin Dagnelie. 1993. Visual stabilization of posture in retinitis pigmentosa and in artificially restricted visual fields. *Investigative ophthalmology & visual science* 34, 10 (1993), 3004–3010.

[48] Sébastien J Villard, Moira B Flanagan, Gina M Albanese, and Thomas A Stoffregen. 2008. Postural instability and motion sickness in a virtual moving room. *Human factors* 50, 2 (2008), 332–345.

[49] Nicholas A Webb and Michael J Griffin. 2003. Eye movement, vection, and motion sickness with foveal and peripheral vision. *Aviation, space, and environmental medicine* 74, 6 (2003), 622–625.

[50] Séamas Weech, Sophie Kenny, and Michael Barnett-Cowan. 2019. Presence and cybersickness in virtual reality are negatively related: a review. *Frontiers in psychology* 10 (2019), 158.

[51] Bing Wu, Teng Leng Ooi, and Zijiang J He. 2004. Perceiving distance accurately by a directional process of integrating ground information. *Nature* 428, 6978 (2004), 73–77.

[52] Fei Wu, George S Bailey, Thomas Stoffregen, and Evan Suma Rosenberg. 2021. Don't Block the Ground: Reducing Discomfort in Virtual Reality with an Asymmetric Field-of-View Restrictor. In *Symposium on Spatial User Interaction*. 1–10.

[53] Fei Wu and Evan Suma Rosenberg. 2019. Combining dynamic field of view modification with physical obstacle avoidance. In *2019 IEEE Conference on Virtual Reality and 3D User Interfaces (VR)*. IEEE, 1882–1883.

[54] Fei Wu and Evan Suma Rosenberg. 2022. Asymmetric Lateral Field-of-View Restriction to Mitigate Cybersickness During Virtual Turns. In *2022 IEEE Conference on Virtual Reality and 3D User Interfaces (VR)*. IEEE, 103–111.